Mono- and di-anionic coordination modes of arylazosalicylates in their bis(η^5-cyclopentadienyl)titanium(IV) complexes: Syntheses and crystal structures

Tushar S. Basu Baul,*[,a] Rajesh Manne,[a] Edward R. T. Tiekink,[,b]**

[a]*Centre for Advanced Studies in Chemistry, North-Eastern Hill University, NEHU Permanent Campus, Umshing, Shillong 793 022, India*

[b]*Research Centre for Crystalline Materials, School of Science and Technology, Sunway University, 47500 Bandar Sunway, Selangor Darul Ehsan, Malaysia*

Abstract

The bis(η^5-cyclopentadienyl)titanium(IV) complexes of 5-[(*E*)-2-(aryl)-1-diazenyl]-2-hydroxybenzoic acids (H_2L^{XASA}) where the aryl group is an X-substituted phenyl ring such that X = CH, COEt, CMe, CF, CCl, CBr and N have been synthesised. Two types of titanium(IV) compounds viz. (i) [Ti(η^5-C_5H_5)$_2$($O_2CC_6H_3$(OH-2)(N=NC_6H_4(H-4)-5))$_2$] (**3**) and [Ti(η^5-C_5H_5)$_2$($O_2CC_6H_3$(OH-2)(N=NC_6H_4(OC_2H_5-4)-5))$_2$] (**4**), and (ii) [Ti(η^5-C_5H_5)$_2$($O_2CC_6H_3$(O-2)(N=NC_6H_4(CH_3-4)-5))] (**5**), [Ti(η^5-C_5H_5)$_2$($O_2CC_6H_3$(O-2)(N=NC_6H_4(F-4)-5))] (**6**), [Ti(η^5-C_5H_5)$_2$($O_2CC_6H_3$(O-2)(N=NC_6H_4(Cl-4)-5))] (**7**), [Ti(η^5-C_5H_5)$_2$($O_2CC_6H_3$(O-2)(N=NC_6H_4(Br-4)-5))] (**8**) and [Ti(η^5-C_5H_5)$_2$($O_2CC_6H_3$(O-2)(N=NC_5H_4(N-4)-5))] (**9**) were isolated and characterised by IR, ^{1}H and ^{13}C NMR spectroscopic techniques. The crystal and molecular

structures of **3**-**9** have been determined by single crystal X-ray crystallography. Compounds **3** and **4** conform to the formula $Cp_2Ti(HL^{XASA}\text{-}\kappa O)_2$ with a monodentate carboxylate ligand while those of **5**-**9** conform to $Cp_2Ti(L^{XASA}\text{-}\kappa^2 O^1,O^2)$ with the dianions chelating the titanium atoms via carboxylate-O and hydroxy-O atoms. The common feature of the molecular structures is the adoption of distorted tetrahedral geometries based $(Cp)_2O_2$ donor sets. Hydroxyl-O–H···O(carbonyl) bonding leads to supramolecular chains in the crystal of **4** but, these are absent in **3**. Persistent Cp-C–H···O(carbonyl) interactions, with the carbonyl atoms accepting two or three such interactions, lead to supramolecular chains with helical (**5**, **7** and **8**) or linear (**6** and **9**) topologies; C–X···π interactions also play an important role in the packing of **6**-**8**.

Keywords: Titanocene complexes, Arylazosalicylates, NMR spectroscopy, Crystal structure

---

* Corresponding author. *E-mail address*: basubaul@nehu.ac.in, basubaulchem@gmail.com (T. S. Basu Baul)

** Additional corresponding author. *E-mail: edwardt@sunway.edu.my* (E.R.T. Tiekink)

1. Introduction

Organometallic and coordination titanium(IV) compounds are of interest due to their reactivity and uses including as reagents for catalytic enantioselective processes [1], organic transformations [2], as initiators for polymerization reactions [3], polymerisation catalysts [4-10] to metal organic frameworks [11-13] and metallo-supramolecular chemistry [14-19]. Other applications include the use of alkoxides or aryloxides precursors for the generation of titanium-based materials [20-26] and their uses as photo-sensitisers and photo-catalysts [27,28], titanium-based drugs [29-39] and cell imaging [40-41]. In recent years, substituted titanium-oxo-clusters, such as those substituted by acetylacetonate, carboxylates and catecholate derivatives, have attracted a great deal of attention, owing to their hydrolytic stability and versatile coordination modes [42-46].

On the other hand, salicylic acid, an ancient anti-inflammatory drug having cancer-fighting properties, has attracted attention for biological applications and shows a great affinity for titanium(IV) ions [47,48]. In spite of the rich chemistry and diverse biological applications of titanocene and titanium(IV) based compounds, the synthetic methodologies are not well established (vide infra) and the number of isolated and structurally characterised titanocene salicylates is scarce. As anticipated, both unsubstituted derivatives, bis(η^5-cyclopentadienyl)titanium(IV) salicylates e.g. [Ti(η^5-C_5H_5)$_2$($O_2CC_6H_4OH$)$_2$] (bis(η^5-cyclopentadienyl)bis(salicylato-κ*O*)titanium(IV)) (**1**) [49], with a monodentate carboxylate ligand, and [Ti(η^5-C_5H_5)$_2$($O_2CC_6H_4O$)] (bis(η^5-cyclopentadienyl)(salicylato-κ^2*O*^{1},*O*^{2})titanium(IV)) (**2**) [50], with a chelating dianion, have been described. Compound **1** has been synthesised by treating Cp_2TiCl_2 with sodium salicylate (1:2 molar ratio) in water containing acetylacetone wherein the role of the latter reagent is not known [49]. In an another

endeavour, compound **2** was prepared from aqueous solutions of Cp_2TiCl_2, salicylic acid and sodium carbonate (1:1.1 molar ratio), the isolation of pure product required meticulous control of the experimental conditions as to minimise hydrolytic side reactions. Additionally, shorter or prolonged reaction times led to the isolation of either unreacted starting materials or oxotitanium(IV) impurities, respectively. In view of the reactions' complexities, both **1** and **2** were reinvestigated [51]. Compound **2** was isolated in high yield (86%) from a reaction containing equivalent amounts of Cp_2TiCl_2, triethylamine and sodium salicylate (generated from NaOH and salicylic acid) in degassed water under stirring conditions for 10 min. The structure of **2** was determined from the results of single crystal X-ray crystallography that confirms the bidentate chelating nature of the doubly deprotonated salicylate ligand [51]. On the other hand, attempted preparations of pure **1** by reacting (i) sodium salicylate and Cp_2TiCl_2 in two different solvents e.g. toluene and water, (ii) salicylic acid and Cp_2TiMe_2 in toluene and (iii) sodium salicylate and acetylacetone treated Cp_2TiCl_2 in water [49] provided either a mixture of **1** and **2** or products could not be separated [51], underscoring the synthetic difficulties in this field.

In spite of such complications, reports on the synthesis of bis(η^5-cyclopentadienyl)titanium(IV) substituted salicylates are available [51,52] but, none of these were characterised crystallographically. In an attempt to design molecules that offer the potential of hydrogen bonding in their supramolecular structures, i.e. ligands such as 2-mercapto-, 3,5-dichloro-2-hydroxy- and 3,5-dinitro-2-hydroxybenzoic acids, these were reacted with Cp_2TiCl_2 in the presence of aquatic β-cyclodextrin polymer in chloroform, which provided high yield of $[Ti(\eta^5\text{-}C_5H_5)_2(O_2CC_6H_4S)\cdot 0.5C_6H_6]$, $[Ti(\eta^5\text{-}C_5H_5)_2(O_2CC_6H_2(3,5\text{-}Cl_2)O)]$ and $[Ti(\eta^5\text{-}C_5H_5)_2(O_2CC_6H_2(3,5\text{-}(NO_2)_2)O)]$; the role of β-cyclodextrin was not fully understood [53]. As a consequence of bidentate chelating nature of salicylates in these compounds, a pseudo-

tetrahedral geometry around titanium(IV) was proposed on the basis of diffraction results. Reports on the synthesis of $[Ti(\eta^5\text{-}(CH_3)C_5H_4)_2(O_2CC_6H_4O)]$ [54], $[Ti(\eta^5\text{-}(CH_3)C_5H_4)_2\{(O_2CC_6H_3\text{-}p\text{-}O)(NN(C_6H_4\text{-}4\text{-}Br))\}]$ [55], $[Ti(\eta^5\text{-}(CH_3)C_5H_4)_2(O_2CC_6H_2(3,5\text{-}(NO_2)_2)O)]$ [56] and $[Ti(\eta^5\text{-}(CH_3)C_5H_4)_2(O_2CC_6H_2(5\text{-}NO_2)_2)O)]$ [57] are also available which were synthesised by reacting $MeCp_2TiCl_2$, aqueous acetylacetone and substituted salicylic acid in chloroform/diethylether mixture but their yields and NMR data are missing. Diffraction data on the isolated crystals conform to a distorted tetrahedral/pseudo-tetrahedral geometry around titanium(IV), as observed previously. The rarity of bis(η^5-cyclopentadienyl)titanium(IV) salicylates can be attributed to the high oxophilic character of titanium cations preventing their crystallisation under ambient conditions and/or in the presence of any oxygenated source (water or adventitious moisture). Moreover, monitoring the kinetics of crystallisation also remains one of the most obvious strategies allowing crystalline materials to be obtained. Recently, the monodentate mode of salicylates in **1** [49] was confirmed from crystallographic data [58]; however, the product was obtained from the reactions of Cp_2TiCl_2, 5-sulfosalicylic acid and salicylic acid in aqueous/chloroform medium wherein the role of 5-sulfosalicylic acid was not explained.

In view of the above technical difficulties and on the basis of previous success with the synthesis and structure determination of titanocene carboxylates of the type $Cp_2Ti(O_2CR)_2$ [59], the present work aimed to synthesise a series of bis(η^5-cyclopentadienyl)titanium(IV) substituted salicylates using a straightforward and reproducible synthetic methodology. For this purpose, 5-[(*E*)-2-(aryl)-1-diazenyl]-2-hydroxybenzoic acids (H_2L^{XASA}, Scheme 1) was used where the aryl group is an X-substituted phenyl ring. The pro-ligand H_2L^{XASA} possesses several interesting features: (i) a flexible carboxylate and phenol groups to endow it with strong coordination

affinity toward titanium ions; (ii) the presence of hydrogen bond donors such as the hydroxyl oxygen and the carboxylate oxygen atoms (and acceptors such as the pyridyl nitrogen) can collaborate in self-assemblies, (iii) the diazenyl group linking a bio-compatible salicylate moiety and the aryl ring can provide additional flexibility to the ligand molecule and (iv) a pyridine ring which provides not only a N-donor atom but also offers rigidity to promote the formation of crystalline products. The pro-ligand H_2L^{XASA} is a salicylic acid derivative functionalised with a aryldiazenyl group and the molecule can function as a mono- $(HL^{XASA})^-$ or dianionic $(L^{XASA})^{2-}$ ligands. In the present contribution, the coordination chemistry of pro-ligand H_2L^{XASA} was explored systematically towards Cp_2TiCl_2 which provided two types of titanium(IV) compounds viz. (a) bis(η^5-cyclopentadienyl)bis(HL^{XASA}-κ*O*)titanium(IV) e.g. $[Ti(\eta^5\text{-}C_5H_5)_2(O_2CC_6H_3(OH\text{-}2)(N{=}NC_6H_4(H\text{-}4)\text{-}5))_2]$ (**3**) and $[Ti(\eta^5\text{-}C_5H_5)_2(O_2CC_6H_3(OH\text{-}2)(N{=}NC_6H_4(OC_2H_5\text{-}4)\text{-}5))_2]$ (**4**), and (b) bis(η^5-cyclopentadienyl)(L^{XASA}-κ^2*O*^{1},*O*^{2})titanium(IV) e.g. $[Ti(\eta^5\text{-}C_5H_5)_2(O_2CC_6H_3(O\text{-}2)(N{=}NC_6H_4(CH_3\text{-}4)\text{-}5))]$ (**5**), $[Ti(\eta^5\text{-}C_5H_5)_2(O_2CC_6H_3(O\text{-}2)(N{=}NC_6H_4(F\text{-}4)\text{-}5))]$ (**6**), $[Ti(\eta^5\text{-}C_5H_5)_2(O_2CC_6H_3(O\text{-}2)(N{=}NC_6H_4(Cl\text{-}4)\text{-}5))]$ (**7**), $[Ti(\eta^5\text{-}C_5H_5)_2(O_2CC_6H_3(O\text{-}2)(N{=}NC_6H_4(Br\text{-}4)\text{-}5))]$ (**8**) and $[Ti(\eta^5\text{-}C_5H_5)_2(O_2CC_6H_3(O\text{-}2)(N{=}NC_5H_4(N\text{-}4)\text{-}5))]$ (**9**). Compounds **3**-**9** were characterised by IR, ^1H and ^{13}C NMR spectroscopic techniques. Further, the crystal and molecular structures of each of the compounds has been determined by single crystal X-ray crystallography.

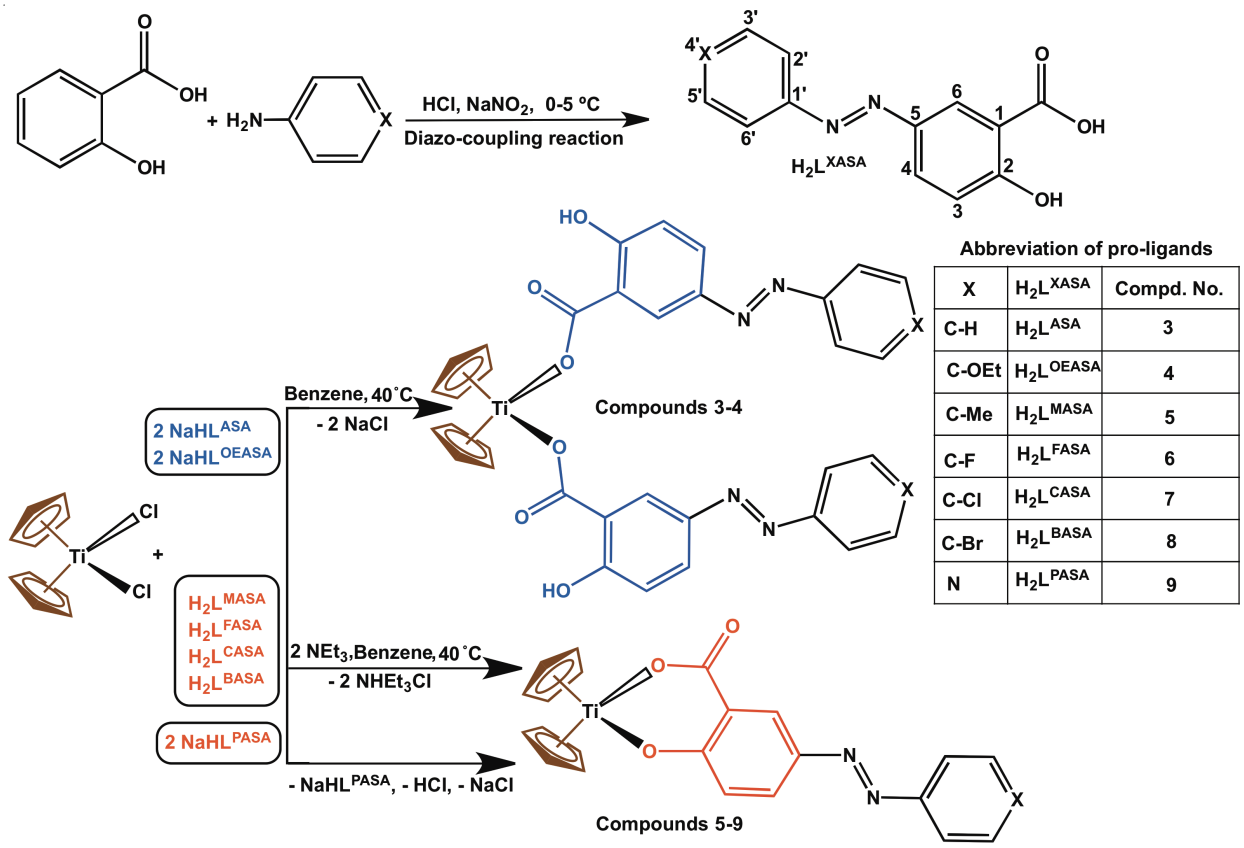

X	H_2L^{XASA}	Compd. No.
C-H	H_2L^{ASA}	3
C-OEt	H_2L^{OEASA}	4
C-Me	H_2L^{MASA}	5
C-F	H_2L^{FASA}	6
C-Cl	H_2L^{CASA}	7
C-Br	H_2L^{BASA}	8
N	H_2L^{PASA}	9

Scheme 1. Synthesis of pro-ligand H_2L^{XASA} and chemical structures of the Ti(IV) compounds **3-9** along with the atom-numbering protocol.

2. Experimental

2.1. Materials and measurements

Aniline (Sd Fine) and *p*-phenetidine (Spectrochem) were freshly distilled and *p*-toludine (Merck) was treated with water/ activated charcoal and recrystallised prior to use, while all other chemicals were used as purchased without purification: bis(η^5-cyclopentadienyl)titanium(IV) dichloride, salicylic acid (Merck), *p*-fluoroaniline, 4-aminopyridine (Spectrochem), *p*-chloroaniline and *p*-bromoaniline (SRL). The solvents used in the reactions were of AR grade

and were dried using standard procedures. Benzene, toluene, hexane and THF were distilled from benzophenone/sodium while methanol was distilled over activated magnesium. Triethylamine was dried over calcium hydride and distilled. All manipulations were performed using standard Schlenk anaerobic lines in an atmosphere of dry dinitrogen or argon, unless otherwise stated. Melting points were measured using a Büchi M-560 melting point apparatus and are uncorrected. IR spectra in the range 4000-400 cm^{-1} were obtained on a Perkin Elmer Spectrum BX series FT-IR spectrophotometer with samples investigated as KBr discs. ^{1}H and ^{13}C NMR spectra were recorded on a Bruker AMX 400 spectrometer at 400.13 and 100.62 MHz, respectively. ^{1}H and ^{13}C chemical shifts were referenced to Me_4Si and $CDCl_3$ set at 0.00 and 77.0 ppm, respectively. *Note: Reactions can be conducted in toluene, however, synthetic conveniences, particularly the higher boiling point of toluene, led to the choice of benzene. Care in handling benzene should be exercised*.

2.2. Synthesis of pro-ligands and sodium salts

Pro-ligands H_2L^{XASA} *viz*. 5-[(*E*)-2-phenyl-1-diazenyl]-2-hydroxybenzoic acid (H_2L^{ASA}), 5-[(*E*)-2-(4-methylphenyl)-1-diazenyl]-2-hydroxybenzoic acid (H_2L^{MASA}), 5-[(*E*)-2-(4-bromophenyl)-1-diazenyl]-2-hydroxybenzoic acid (H_2L^{BASA}) [60], 5-[(*E*)-2-(4-chlorophenyl)-1-diazenyl]-2-hydroxybenzoic acid (H_2L^{CASA}) [61], 5-[(*E*)-2-(4-pyridyl)-1-diazenyl]-2-hydroxybenzoic acid (H_2L^{PASA}) [62] were prepared starting from salicylic acid and the corresponding aniline using conventional diazonium salt chemistry, in accordance with literature procedures. Synthetic and spectral details for the pro-ligands 5-[(*E*)-2-(4-ethoxyphenyl)-1-diazenyl]-2-hydroxybenzoic acid (H_2L^{OEASA}) and 5-[(*E*)-2-(4-fluorophenyl)-1-diazenyl]-2-hydroxybenzoic acid (H_2L^{FASA}) are described below.

2.2.1. Synthesis of 5-[(E)-2-(4-ethoxyphenyl)-1-diazenyl]-2-hydroxybenzoic acid (H_2L^{OEASA})

An analogous method to that used for the preparation of H_2L^{ASA} [60] was followed using *p*-phenetidine (5.00 g, 36.44 mmol) and salicylic acid (5.02 g, 35.85 mmol). The yellow reaction mixture was acidified with dilute acetic acid and the obtained precipitate was washed with water and dried. The crude product was washed with hexane to remove any tarry materials and recrystallised from methanol to yield orange crystalline material of H_2L^{OEASA}. Yield: 6.72 g, 64%. M. p.: 190-192 ˚C. Anal. found: C, 62.80; H, 4.80; N, 10.03. Calcd for $C_{15}H_{14}N_2O_4$: C, 62.93; H, 4.93; N, 9.79%. IR absorptions (cm^{-1}): 1656 $\nu(OCO)_{asym}$, 1600, 1581, 1478, 1460, 1250, 1221, 1140, 840, 767, 520, 468. ^1H NMR (DMSO-d_6/$CDCl_3$) δ_H: 8.34 [d, 2.1 Hz, 1H, H-6], 7.95 [dd, 9.0 & 2.1 Hz, 1H, H-4], 7.78 [XX' portion of AA'XX', 2H, H-3' & H-5'], 6.97 [d, 9.0 Hz, 1H, H-3], 6.91 [AA' portion of AA'XX', 2H, H-2' & H-6'], 4.62 [brs, 1H, OH], 4.04 [q, 2H, CH_2], 1.37 [t, 3H, CH_3]. Signal for the carboxylic acid were exchanged due to presence of water in the solvent. $^{13}C\{^1H\}$ NMR (DMSO-d_6/$CDCl_3$) δ_C: 172.54 [COO], 163.72 [C-2], 161.02 [C-1'], 146.54 [C-5], 145.20 [C-4'], 128.16 [C-4], 126.78 [C-6], 124.35 [C-3' & C-5'], 117.94 [C-3], 114.54 [C-2' & C-6'], 112.82 [C-1], 63.67 [CH_2], 14.64 [CH_3].

2.2.2. Synthesis of 5-[(E)-2-(4-fluorophenyl)-1-diazenyl]-2-hydroxybenzoic acid (H_2L^{FASA})

An analogous method to that used for the preparation of H_2L^{CASA} [61] was followed using *p*-fluroaniline (5.0 g, 45.02 mmol) and salicylic acid (6.21 g, 45.02 mmol). The yellow reaction mixture was acidified with dilute acetic acid and the obtained precipitate was washed with water and dried. The crude product was washed with hexane to remove any tarry materials and recrystallised from methanol to yield yellow microcrystalline product of H_2L^{CASA}. Yield: 6.72 g, 57%. M. p.: 235-236 ˚C. Anal. found: C, 59.80; H, 4.10; N, 10.93. Calcd for $C_{13}H_9FN_2O_3$: C, 60.00; H, 3.49; N, 10.77%. IR absorptions (cm^{-1}): 1665 $\nu(OCO)_{asym}$,1616, 1575, 1477, 1455, 1395, 1379, 1311, 1217, 1201, 1178, 1078, 1065, 1009, 897, 840, 829, 708, 663,

567, 469. ^{1}H NMR (DMSO-d_6/$CDCl_3$) δ_H; 11.65 [brs, 1H, COOH], 8.39 [d, 1H, H-6], 7.97 [dd, 1H, H-4], 7.81 [XX' portion of AA'XX', 2H, H-3' & H-5'], 7.11 [AA' portion of AA'XX', 2H, H-2' & H-6'], 7.00 [d, 9.0 Hz, 1H, H-3], 6.14 [brs,1H, OH]. $^{13}C\{^{1}H\}$ (DMSO-d_6/$CDCl_3$) δ_H: 172.11 [COO], 165.17 and 162.67 [C-4', (^{13}C-^{19}F = 251 Hz)], 164.29 [C-2], 148.86 [C-1'], 144.87 [C-5], 128.20 [C-4], 127.33 [C-6], 124.52 and 124.44 [C-3' & C-5', (^{13}C-^{19}F = 8.0 Hz)], 118.05 [C-3], 115.99 and 115.76 [C-2' & C-6', (^{13}C-^{19}F = 23 Hz)], 113.02 [C-1].

Sodium salts viz. sodium 5-[(*E*)-2-(phenyl)-1-diazenyl]-2-hydroxybenzoate ($NaHL^{ASA}$) [60] and sodium 5-[(*E*)-2-(4-pyridyl)-1-diazenyl]-2-hydroxybenzoate ($NaHL^{PASA}$) [62] were prepared by the method described earlier. An analogous method to that used for the preparation of $NaHL^{ASA}$ [60] was followed for the preparation of sodium 5-[(*E*)-2-(4-ethoxyphenyl))-1-diazenyl]-2-hydroxybenzoate ($NaHL^{OEASA}$). Dark-red powder; M. p.: > 350 ˚C. IR absorptions (cm^{-1}): 1600 $\nu(OCO)_{asym}$, 1585, 1493, 1484, 1464, 1441, 1367, 1317, 1292, 1257, 1176, 1141, 1026, 834, 767, 691, 575.

2.3. Synthesis of titanocene compounds ***3-9***

2.3.1. Synthesis of $[Ti(\eta^5\text{-}C_5H_5)_2(O_2CC_6H_3(OH\text{-}2)(N{=}NC_6H_4(H\text{-}4)\text{-}5))_2]$ ***(3)***

A freshly prepared solution of titanocene dichloride (0.100 g, 0.401 mmol) in anhydrous benzene (15 ml) was added to a stirred suspension of $NaHL^{ASA}$ (0.230 g, 0.883 mmol) in anhydrous benzene (15 ml) and the stirring was continued at 40 ˚C for 4 h. The dark-red reaction mixture was evaporated to dryness, washed with hot hexane and dried in vacuo. The residue was extracted into hot anhydrous chloroform (20 ml) and filtered through a frit covered with pre-dried neutral silica (3 cm layer, mesh size 100-200) and eluted further with anhydrous chloroform (3 x 1 ml). The clear red filtrate was concentrated using a rotary evaporator to around

3 ml, which upon standing overnight afforded orange crystals of **3** at ambient temperature. Crystals were washed with a small amount of benzene and dried in vacuo. Yield: 0.15 g, 56 %. M. p.: 180-183 ˚C. Anal. found: C, 65.20; H, 4.12; N, 9.03. Calcd for $C_{36}H_{28}N_4O_6Ti$: C, 65.46; H, 4.27; N, 8.48%. IR absorptions (cm^{-1}): 1633 $\nu(OCO)_{asym}$, 1593, 1570, 1484, 1417, 1384, 1356, 1295, 1251, 1174, 824, 802, 766, 684, 462. ^1H NMR ($CDCl_3$) δ_H: 12.32 [s, 2H, OH], 8.37 [d, 2H, H-6], 7.82 [m, 4H, H-2' & H-6'], 7.35-7.43 [m, 4H, H-4 & H-4'], 7.22 [m, 4H, H-3' & H-5'], 6.98-7.03 [m, 2H, H-3], 6.70 [s, 10H, C_5H_5]. $^{13}C\{^1H\}$ NMR ($CDCl_3$) δ_C: 175.52 [COO], 163.82 [C-2], 151.84 [C-1'], 145.04 [C-5], 130.18 [C-4'], 129.02 [C-4], 128.47 [C-3' & C-5'], 127.38 [C-6], 122.59 [C-2' & C-6'], 119.41 [C_5H_5], 117.87 [C-3], 115.52 [C-1].

*2.3.2. Synthesis of [Ti(η^5-C_5H_5)$_2$($O_2CC_6H_3$(OH-2)(N=NC_6H_4(OC_2H_5-4)-5))$_2$] (**4**)*

Two synthetic procedures are described below.

Method 1: An analogous method to that used for the preparation of **3** was followed using titanocene dichloride (0.100 g, 0.401 mmol) and $NaHL^{OEASA}$ (0.256 g, 0.832 mmol) except that the reaction mixture was directly filtered and washed with benzene. Red-orange crystals were washed with small amount of hexane and dried in vacuo. Yield: 0.19 g, 64 %. M. p.: 171-173 ˚C. Anal. found: C, 64.50; H, 4.18; N, 7.40. Calcd for $C_{40}H_{36}N_4O_8Ti$: C, 64.18; H, 4.85; N, 7.48%. IR absorptions (cm^{-1}): 1631 $\nu(OCO)_{asym}$, 1604, 1582, 1499, 1477, 1392, 1335, 1247, 1216, 923, 825, 774, 462, 517. ^1H NMR ($CDCl_3$) δ_H: 12.25 [s, 2H, OH], 8.32 [d, 2H, H-6], 7.80 [XX' portion of AA'XX', 4H, H-3' & H-5'], 7.35 [AA' portion of AA'XX', 4H, H-2' & H-6'], 6.90-7.02 [m, 4H, H-3 & H-4], 6.69 [s, 10H, C_5H_5], 4.01 [q, 4H, CH_2], 1.37 [t, 6H, CH_3]. $^{13}C\{^1H\}$ NMR ($CDCl_3$) δ_C: 175.64 [COO], 163.31 [C-2], 160.78 [C-1'], 146.23 [C-5], 145.19 [C-4'], 128.04 [C-4], 127.15 [C-6], 124.43 [C-3' & C-5'], 119.41 [C_5H_5], 119.27 [C-2' & C-6'], 114.65 [C-3], 114.10 [C-1], 63.67 [CH_2], 14.78 [CH_3].

Method 2: A freshly prepared solution of titanocene dichloride (0.10 g, 0.40 mmol) in anhydrous benzene (15 ml) was added to a stirred solution of H_2L^{OEASA} (0.23 g, 0.80 mmol) in anhydrous benzene (15 ml). Subsequently to the clear reaction mixture, a benzene solution (10 ml) of NEt_3 (0.080 g, 0.79 mmol) was added drop-wise where upon the wine-red solution turns dark-red along with precipitation of $Et_3N{\cdot}HCl$. The reaction mixture was slowly heated to 40 ˚C and stirring was continued for an additional 4 h. The dark-red solution was filtered through a frit covered with pre-dried neutral silica (3 cm layer, mesh size 100-200) and eluted with anhydrous benzene (3 x 1 ml). The clear filtrate was concentrated using a rotary evaporator to around 3 ml, which upon standing overnight afforded red-orange crystals of **4** at ambient temperature. Crystals were washed with small amount of anhydrous hexane and dried in vacuo. Yield: 0.17 g, 53%. M. p.: 171-173 ˚C. Spectroscopic data of the compound closely match with that reported for **4** synthesised by method 1.

*2.3.3. Synthesis of [Ti(η^5-C_5H_5)$_2$($O_2CC_6H_3$(O-2)(N=NC_6H_4(CH_3-4)-5))] (**5**)*

A freshly prepared solution of titanocene dichloride (0.100 g, 0.401 mmol) in anhydrous benzene (20 ml) was added to a clear stirred solution of H_2L^{MASA} (0.102 g, 0.401 mmol) in anhydrous benzene (50 ml). Subsequently, to a clear reaction mixture, a benzene solution (10 ml) of NEt_3 (0.080 g, 0.790 mmol) was added drop-wise where upon the wine-red solution turned dark-red along with precipitation of $Et_3N{\cdot}HCl$. The reaction mixture was slowly heated to 40 ˚C and stirring was continued for additional 4 h. The dark-red solution was filtered through a frit covered with pre-dried neutral silica (3 cm layer, mesh size 100-200) and eluted with anhydrous benzene (3 x 1 ml). The clear filtrate was concentrated using a rotary evaporator to around 15 ml, which upon standing for a week afforded dark-red crystals of **5** at ambient temperature. Crystals were washed with small amount of anhydrous benzene and dried in vacuo. Yield: 0.13 g, 74 %.

M. p.: 150-152 ˚C. Anal. found: C, 67.10; H, 4.19; N, 7.80. Calcd for $C_{24}H_{20}N_2O_3Ti$: C, 66.68; H, 4.66; N, 6.48%. IR absorptions (cm^{-1}): 1614 $\nu(OCO)_{asym}$, 1598, 1472, 1414, 1310, 1248, 1175, 1128, 1128, 822, 644, 501. ^1H NMR ($CDCl_3$) δ_H: 8.45 [d, 1H, H-6], 8.06 [dd, 1H, H-4], 7.74 [XX' portion of AA'XX', 2H, H-3' & H-5'], 7.25 [AA' portion of AA'XX', 2H, H-2' & H-6'], 7.05 [d, 1H, H-3], 6.60 [s, 10H, C_5H_5], 2.37 [t, 3H, CH_3]. $^{13}C\{^1H\}$ NMR ($CDCl_3$) δ_C: 173.89 [COO], 165.49 [C-2], 151.84 [C-1'], 146.51 [C-5], 142.56 [C-4'], 131.12 [C-3' & C-5'], 129.65 [C-4], 128.49 [C-6], 123.95 [C-2' & C-6'], 121.69 [C_5H_5], 119.44 [C-3], 114.45 [C-1], 22.84 [CH_3].

*2.3.4. Synthesis of [Ti(η^5-C_5H_5)$_2$($O_2CC_6H_3$(O-2)(N=NC_6H_4(F-4)-5))] (**6**)*

An analogous method to that used for the preparation of **5** was followed using titanocene dichloride (0.100 g, 0.401 mmol), H_2L^{FASA} (0.113g, 0.401 mmol) and Et_3N (0.080 g, 0.790 mmol). The clear filtrate was concentrated using a rotary evaporator to around 15 ml, which upon standing overnight afforded dark-red crystals of **6** at ambient temperature. Crystals were washed with small amount of anhydrous benzene and dried in vacuo. Yield: 0.12 g, 68 %. M. p.: 187-189 ˚C. Anal. found: C, 63.40; H, 3.59; N, 6.10. Calcd for $C_{23}H_{17}FN_2O_3Ti$: C, 63.32; H, 3.93; N, 6.42%. IR absorptions (cm^{-1}): 1622 $\nu(OCO)_{asym}$, 1597, 1497, 1471, 1450, 1417, 1308, 1247, 1225, 1166, 1129, 1019, 837, 823, 497. ^1H NMR ($CDCl_3$) δ_H: 8.40 [d, 1H, H-6], 7.98 [dd, 1H, H-4], 7.82 [XX' portion of AA'XX', 2H, H-3' & H-5'], 7.11 [AA' portion of AA'XX', 2H, H-2' & H-6'], 6.99 [d, 1H, H-3], 6.53 [s, 10H, C_5H_5]. $^{13}C\{^1H\}$ NMR ($CDCl_3$) δ_C: 175.18 [COO], 167.96 and 165.42 [C-4', (^{13}C-^{19}F = 255 Hz)], 167.04 [C-2], 151.63 [C-1'], 147.61 [C-5], 130.95 [C-4], 130.10 [C-6], 127.28 and 127.20 [C-3' & C-5', (^{13}C-^{19}F = 8.0 Hz)], 122.94 [C_5H_5], 120.81[C-3], 118.76 and 118.53 [C-2' & C-6'], 115.75 [C-1].

2.3.5. Synthesis of [Ti(η^5-C_5H_5)$_2$($O_2CC_6H_3$(O-2)(N=NC_6H_4(Cl-4)-5))] (7)

An analogous method to that used for the preparation of **5** was followed using titanocene dichloride (0.100 g, 0.401 mmol), H_2L^{CASA} (0.117 g, 0.401 mmol) and Et_3N (0.080 g, 0.790 mmol)). The turbid reaction mixture was filtered; filtrate was concentrated to dryness using a rotary evaporator. The brick-red residue was washed with anhydrous hexane and dried in vacuo. The solid material was dissolved in anhydrous chloroform (15 ml), filtered through a frit which upon standing overnight afforded dark-red crystals of **7** at ambient temperature. Crystals were washed with small amount of anhydrous benzene and dried in vacuo. Yield: 0.13 g, 71 %. M. p.: 148-150 ˚C. Anal. found: C, 60.68; H, 3.70; N, 6.30. Calcd for $C_{23}H_{17}ClN_2O_3Ti$: C, 61.02; H, 3.78; N, 6.19%. IR absorptions (cm^{-1}): 1629 $\nu(OCO)_{asym}$,1598, 1499, 1467, 1499, 1412, 1311, 1248, 1175, 1125, 1043, 821, 658, 466. ^1H NMR ($CDCl_3$) δ_H: 8.42 [d, 1H, H-6], 8.00 [dd, 1H, H-4], 7.77 [XX' portion of AA'XX', 2H, H-3' & H-5'], 7.38 [AA' portion of AA'XX', 2H, H-2' & H-6'], 7.00 [d, 1H, H-3], 6.54 [s, 10H, C_5H_5]. $^{13}C\{^1H\}$ NMR ($CDCl_3$) δ_C: 175.05 [COO], 167.17 [C-2], 153.39 [C-1'], 147.55 [C-5], 138.90 [C-4'], 131.88 [C-3' & C-5'], 130.94 [C-4], 130.26 [C-6], 126.50 [C-2' & C-6'], 122.89 [C_5H_5], 120.80 [C-3], 115.75 [C-1].

*2.3.6. Synthesis of [Ti(η^5-C_5H_5)$_2$($O_2CC_6H_3$(O-2)(N=NC_6H_4(Br-4)-5))] (**8**)*

An analogous method to that used for the preparation of **5** was followed using titanocene dichloride (0.100 g, 0.401 mmol), H_2L^{BASA} (0.117 g, 0.401 mmol) and Et_3N (0.080 g, 0.790 mmol)). The turbid reaction mixture was filtered; filtrate was concentrated to dryness using a rotary evaporator. The brick-red residue was washed with anhydrous hexane and dried in vacuo. The solid material was dissolved in anhydrous chloroform (30 ml), filtered through a frit, which upon standing for three days afforded dark-red crystals of **8** at ambient temperature. Crystals were washed with small amount of anhydrous benzene and dried in vacuo. Yield: 0.11 g, 55 %. M. p.: 150-152 ˚C. Anal. found: C, 56.10; H, 3.40; N, 5.30. Calcd for $C_{23}H_{17}BrN_2O_3Ti$: C, 55.56;

H, 3.45; N, 5.63%. IR absorptions (cm^{-1}): 1629 $\nu(OCO)_{asym}$, 1618, 1599, 1449, 1472, 1413, 1393, 1309, 1261, 1248, 1171, 1127, 1065, 1024, 818, 707, 567, 472. ^{1}H NMR ($CDCl_3$) δ_H: 8.42 [d, 1H, H-6], 7.99 [dd, 1H, H-4], 7.69 [XX' portion of AA'XX', 2H, H-3' & H-5'], 7.56 [AA' portion of AA'XX', 2H, H-2' & H-6'], 7.00 [d, 1H, H-3], 6.53 [s, 10H, C_5H_5]. $^{13}C\{^{1}H\}$ NMR ($CDCl_3$) δ_C: 175.36 [COO], 167.53 [C-2], 154.07 [C-1'], 147.88 [C-5], 135.16 [C-3' & C-5'], 131.26 [C-4'], 130.64 [C-4], 127.70 [C-6], 127.07 [C-2' & C-6'], 123.21 [C_5H_5], 121.14 [C-3], 116.07 [C-1].

*2.3.7. Synthesis of [Ti(η^5-C_5H_5)$_2$($O_2CC_6H_3$(O-2)(N=NC_5H_4(N-4)-5))] (**9**)*

An analogous method to that used for the preparation of **3** was followed using titanocene dichloride (0.100 g, 0.401 mmol) and excess $NaHL^{PASA}$ (0.230 g, 0.883 mmol). The resulting dark-red suspension was evaporated to dryness, washed with hot hexane and dried in vacuo. The residue was extracted into hot anhydrous dichloromethane (30 ml) and filtered through a frit covered with pre-dried neutral silica (3 cm layer, mesh size 100-200) and eluted further with anhydrous dichloromethane (3 x 1 ml). The clear red filtrate was concentrated using a rotary evaporator to around 20 ml, which upon standing overnight afforded fine dark-red crystals of **9** at ambient temperature. Crystals were dissolved by boiling in dichloromethane/DMF (20 ml/1ml, v/v) and the clear solution was concentrated to 10 ml, which upon standing at ambient temperature for about an hour afforded X-ray quality crystals. Crystals were washed with small amount of benzene and dried in vacuo. Yield: 0.13 g, 77 %. M. p.: 328-330 ˚C. Anal. found: C, 63.50; H, 4.50; N, 10.26. Calcd for $C_{22}H_{17}N_3O_3Ti$: C, 63.02; H, 4.09; N, 10.02%. IR absorptions (cm^{-1}): 1617 $\nu(OCO)_{asym}$, 1590, 1465, 1419, 1309, 1253, 1174, 1122, 825, 790, 603. ^{1}H NMR ($CDCl_3$/DMSO-d_6) δ_H: 8.76 [d, 1H, H-6], 8.70 [XX' portion of AA'XX', 2H, H-3' & H-5'], 7.97 [dd, 1H, H-4], 7.63 [AA' portion of AA'XX', 2H, H-2' & H-6'], 6.74 [d, 1H, H-3], 6.45 [s, 10H, C_5H_5]. $^{13}C\{^{1}H\}$ NMR ($CDCl_3$/DMSO-d_6) δ_C: 170.57 [COO], 168.98 [C-2], 156.96 [C-1'], 150.60

[C-3' & C-5'], 144.63 [C-5], 130.50 [C-4], 126.03 [C-6], 120.25 [C-3], 120.01 [C-1], 119.18 [C_5H_5], 115.77 [C-2' & C-6'].

*2.4. Single crystal X-ray structure determinations of **3-9***

Crystals of compounds **3**, **7**, **8** (chloroform), **4** and **6** (benzene), **5** (benzene/THF; 2/1 v/v) and **9** (dichloromethane/DMF; 20/1 v/v) suitable for single-crystal X-ray diffraction analysis were grown from the respective solutions by slow solvent evaporation at room temperature. Intensity data for compounds **3-9** were measured at room temperature on an Agilent Xcalibur Eos Gemini diffractometer equipped with a CCD area detector and graphite-monochromated Mo Kα radiation (λ = 0.71073 Å); Cu Kα radiation (λ = 1.54184 Å) was employed for **5**. Data reduction and empirical absorption corrections, based on a multi-scan technique, were applied [63]. Each structure was solved by direct methods [64] and refined on F^2 with anisotropic displacement parameters and C-bound H atoms in the riding model approximation [65]. For **3** and **4**, the hydroxyl-O–H atoms were located from difference maps but, were refined with the distance restraint O–H = 0.82±0.01 Å. A weighting scheme of the form $w = 1/[\sigma^2(F_o^2) + (aP)^2 + bP]$ where $P = (F_o^2 + 2F_c^2)/3)$ was introduced for each refinement. The structures were determined at room temperature and uniformly featured high displacement parameters, in particular for the cyclopentadienyl (Cp) groups. However, the structures were determined unambiguously and are entirely consistent with the spectroscopic data. In the refinement of **3**, the (-1 0 4), (-1 0 3), (4 1 3) and (0 2 6) reflections were omitted from the final cycles of refinement owing to poor agreement. In **6**, the C17 atom was restrained to be nearly isotropic. The (2 0 4) reflection was omitted from the refinement of **7**. In **7**, the maximum and minimum residual electron density peaks of 1.17 and 0.45 eÅ^{-3} were located 1.45 and 0.72 Å from the C5 and Cl1 atoms, respectively. The crystal of **8** was a two-component twin [twin law: 1 0 0.382 0 -1 0 0 0 -1] with the minor component

comprising 0.343(5) of the sample. Crystal data and refinement details are collected in Table 1. The molecular structure diagrams were generated by ORTEP for Windows [66] at the 25% probability level and the packing diagrams with DIAMOND [67]. Additional data analysis was made with PLATON [68].

3. Results and discussion

*3.1. Synthesis and spectroscopic characterisation of compounds **3-9***

The paucity of bis(η^5-cyclopentadienyl)titanium(IV) salicylates is mainly due to the high oxophilic character of Ti-cations, preventing them to crystallise under ambient conditions and/or in the presence of any oxygenated source. In view of this, the primary objective herein was set to standardise the synthetic procedure and secondly to crystallise the powder/ microcrystalline materials to obtain X-ray quality single crystals to enable the determination of their hitherto unknown molecular structures. In the current investigation, titanocene arylazosalicylates **3** and **4** were synthesised by the reactions of titanocene dichloride with two molar equivalents of the freshly prepared corresponding sodium salts of the respective pro-ligands in benzene at 40 ˚C under stirring. As a representative case, attempted reaction of titanocene dichloride, H_2L^{OEASA} and NEt_3 using 1:2:2 molar ratio in benzene also afforded compound **4**. However, the cumbersome workup procedure was detrimental to the overall yield and thus synthetic success led to the choice of sodium salt method. On the other hand, **5-8** were prepared by the reactions of titanocene dichloride with the respective pro-ligands in benzene in the presence of triethylamine in 1:1:2 molar proportions (Scheme 1). As an exception, by adopting the analogous methodology, compound **9** could not be isolated owing to the insolubility of H_2L^{PASA}, nevertheless the reaction of titanocene dichloride with excess $NaHL^{PASA}$ (1:2 molar proportions) proceeded smoothly in benzene (refer to the Experimental section for details). The final yields of the products were >50%

which were dependent on the workup conditions applied for the purification and recovery of the crystals. Crystalline samples of the compounds **3-9** can be stored for several months in an inert environment; of these compounds **3-5** and **9** retain their colour, lustre and melting points. However, compounds **4-6** turns into powder with time but retain their original melting points. The compounds were characterised by NMR, IR spectroscopy and by single-crystal X-ray crystallography.

The IR spectra of **3-9** show two intense bands in the regions between 1633-1617 and 1417-1384 cm^{-1} corresponding to $\nu(OCO)_{asym}$ and $\nu(OCO)_{sym}$ vibrations, respectively. The observed differences between the asymmetric and symmetric vibrations are >200 cm^{-1}; suggesting a monodentate coordination of the carboxylate ligand [69]; this assumption was subsequently confirmed from the results of single crystal X-ray diffraction studies (see section 3.2). Since the titanocene arylazosalicylates in the present investigation were generated from solution methods, it was therefore necessary to confirm the purity of the bulk material and also to comprehend the solution behaviour of **3-9.** For this purpose, solution-state ^{1}H and $^{13}C\{^{1}H\}$ NMR studies were undertaken using vacuum dried crystalline samples of **3-9** that were dissolved in $CDCl_3$. All the samples confirm the purity and displayed the expected signals due to the carboxylate and Cp ligands, and the integration values in the spectra are in agreement with those expected for the structure types $Cp_2Ti(HL^{XASA}\text{-}\kappa O)_2$ (**3** and **4**) and $Cp_2Ti(L^{XASA}\text{-}\kappa^2 O^1,O^2)$ (**5-9**) as shown in Scheme 1 (refer to Figs S1-S14 for ^{1}H and $^{13}C\{^{1}H\}$ NMR spectra). NMR solutions of the compounds prepared under dinitrogen/ argon were found to be stable for at least two hours but, tended to decompose slowly. Compounds **3** and **4** displayed a singlet at around 12.3 ppm due to phenolic OH which is absent in rest of the compounds, corroborating that the ligand bonds to titanium(IV) via carboxylate oxygen atom while in **5-9** the di-anionic ligand chelate the titanium

atom via carboxylate-O and hydroxy-O atoms. Two chemically equivalent Cp rings were detected as sharp singlet in the range 6.53-6.70 ppm in the ^{1}H NMR spectra while a single signal was observed between 119.2 and 123.2 ppm in the ^{13}C NMR spectra. The carboxylate carbonyl-carbon resonances for the compounds **3**-**8** were observed at δ 175 ppm and for compound **9** at 170.6 ppm. As such, no sign of decomposition was noticed in NMR spectra after dissolution of the crystalline samples, confirming that the solid-state structures were retained in solution at least for two hours. The subtle changes in the ligand substitution did not affect the general pattern of the NMR spectra and the observed signals were generally broad and unresolved which prevented the measurement of coupling constants.

*3.2. Description of the crystal and molecular structures of **3**-**9***

The molecular structures of **3**-**9** are illustrated in Fig. 1 and selected geometric parameters for the seven structures are collated in Table 2. Each crystal is solvent-free and comprises a single molecule in the asymmetric unit. The structures fall into two classes, with **3** and **4** having the general formula $Cp_2Ti(HL^{XASA}\text{-}\kappa O)_2$, and those of **5**-**9** conforming to $Cp_2Ti(L^{XASA}\text{-}\kappa^2O^1,O^2)$. The difference arises as in the latter series, the hydroxyl group of the carboxylate ligand is also deprotonated leading to a dianion so that each complex features a titanium(IV) centre.

In **3**, the titanium atom is coordinated by two oxygen atoms derived from two monodentate hydroxylbenzoate ligands. This is confirmed by the observation that the C–O1, O3 bond lengths are 0.03-0.04 Å longer than the C=O2, O4 bond lengths and that the carbonyl-O2 and O4 atoms are approximately 3.5 Å distant from the titanium centre. Intramolecular hydroxyl-O–H···O(carbonyl) hydrogen bonds close S(6) loops, Table 3, and confer co-planarity to the carboxyl and attached phenyl rings, with the CO_2/C_6 dihedral angles being 5.1(8) and 3.9(8)° for the O1- and O4- carboxylate ligands, respectively. The dihedral angle between the CO_2/CO_2

planes is 23.4(8)°, indicating a non-planar relationship. The coordination geometry is best described as pseudo-tetrahedral the two η^5-cyclopentadienyl (Cp) anions assumed to occupy a single position each. The Ti–O1, O4 bond lengths are experimentally equivalent. While the Ti–C(Cp) bond lengths span an experimentally distinct range of 2.332(5) to 2.397(5) Å, no pattern to the variations are apparent. Indeed, the Ti···Cg ring centroid distances of 2.049(3) and 2.058(3) Å suggest any differences are not chemically significant. The tetrahedral angles range from a narrow 90.24(12)°, for O1–Ti–O4, to a broad 131.69(12)°, subtended by the more bulky Cp rings. The O1-carboxylate ligand is close to co-planar with the dihedral angle between the aromatic residues being 2.5(3)° but, the O4-carboxylate ligand is twisted with the equivalent angle being 15.6(2)°. The molecular structure of **4** presents very similar features as for **3**. The carboxylate residues tend to be more co-planar with the CO_2/CO_2 dihedral angle being 13.2(3)° but, greater twists are noted between the CO_2/C_6 planes, i.e. 6.1(4) and 11.85(14)° for the O1- and O4-carboxylate ligands, respectively, even though the intramolecular hydroxyl-O–H···O(carbonyl) hydrogen bonds persist, Table 3. The dihedral angle between the aromatic residues in each ligand is similar, i.e. 10.60(10) and 7.23(7)°.

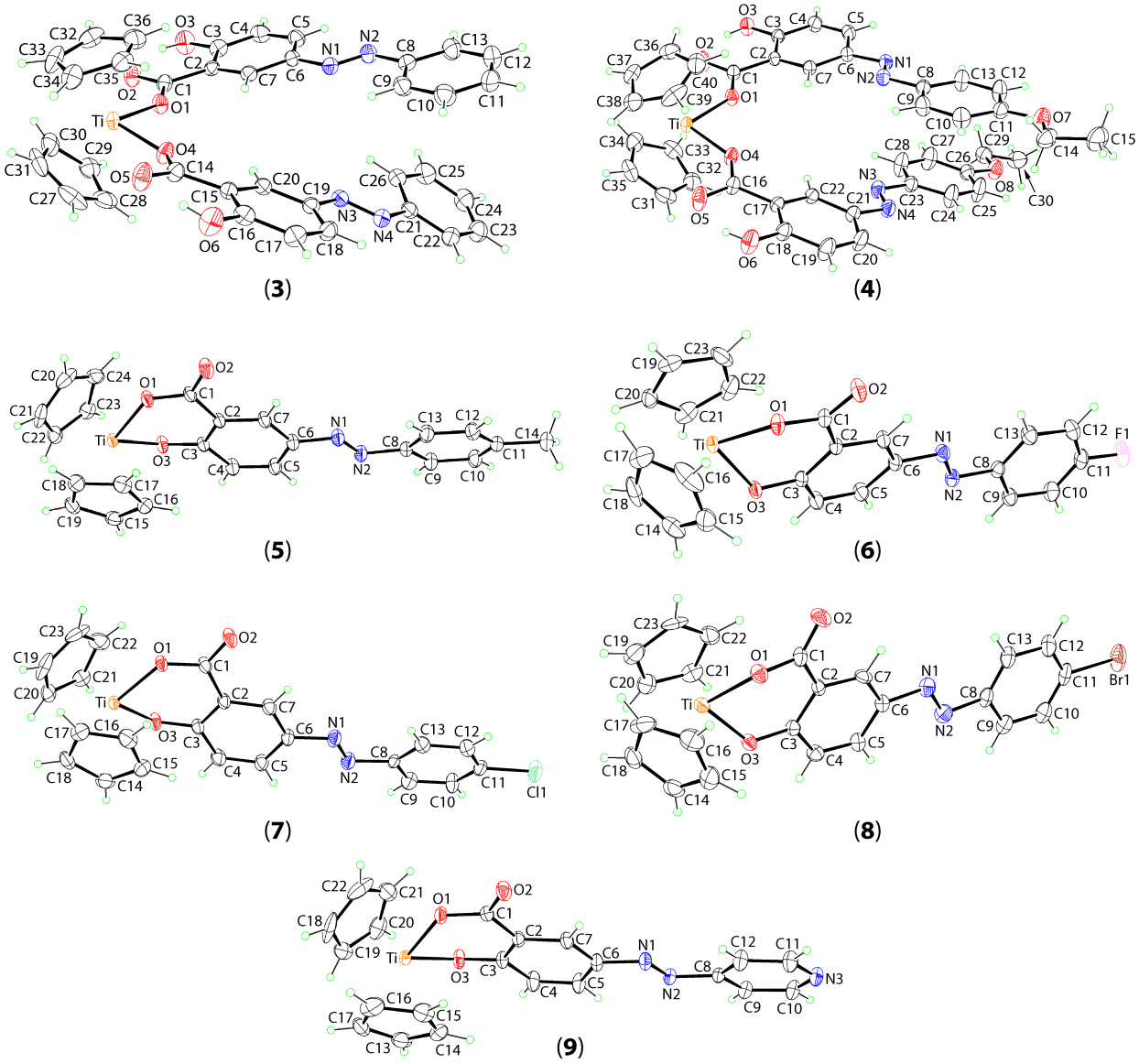

Fig. 1. Molecular structures of **3**-**9**, showing atom labelling schemes and displacement ellipsoids at the 25% probability level.

The molecular structures of **5**-**9** are very similar to each other. In **5**, the titanium atom is chelated by the carboxylate-O1 and hydroxyl-O3 atoms with the former bond being about 0.05 Å longer, an observation correlated with the influence of the proximate electronegative carbonyl-O2

atom; the C1–O1, O2 distances of 1.295(3) and 1.221(3) Å are significantly different in accord with expectation. The six-membered chelate ring is not planar and is best described as being based on a half-chair with the titanium atom lying 0.592(2) Å above the least-squares plane through the O1,O3,C1-C3 atoms [r.m.s. deviation = 0.054 Å]. The coordination geometry is distorted tetrahedral within a C_2O_2 donor set as described above. The O1–Ti–O3 chelate angle is a little more acute than the O1–Ti–O4 angles in **3** and **4**, and the average Ti–C(Cp) bond lengths tend to be a little longer, Table 2. The angle between the carboxylate and phenyl rings is 8.1(3)°, and the angle between aromatic residues 15.83(12)°. Essentially the same molecular structures are noted for **6**-**9**. The structures of **6** and **7** exhibit the maximum [0.699(2) Å] and minimum [0.567(6) Å] deviations of the titanium atom from the chelate ring. The dihedral angle between the CO_2/C_6 planes is minimum in **6**, i.e. 1.9(4)°, and the maximum twist in the carboxylate ligands is seen in **9**, i.e. 18.01(14)°.

As discussed in a recent contribution [59], the structural motif observed for **3** and **4** conforms with expectation for the approximately 25 compounds of the general formula $Cp_2Ti(O_2CR)_2$. By contrast, an evaluation of the crystallographic literature [70] shows there are only five precedents for Cp_2Ti(salicylate derivatives), which exhibit very similar structural features with one notable exception. In the structure of the parent compound, Cp_2Ti(salicylate) [51], the chelate ring is somewhat more planar than reported for other derivatives and for the structures described herein. Thus, the titanium atom lies 0.4180(11) above the remaining five atoms of the chelate ring with the maximum deviation from the plane being 0.019(6) Å for the C1 atom.

In the crystal of **3**, π···π stacking interactions predominate, Table 3. Thus, connections between Cp and hydroxylbenzoate rings, and between hydroxylbenzoate and phenyl rings of like

molecules connect molecules into a supramolecular layer parallel to (0 1 1), Fig. 2a. Layers stack without directional interactions between them as shown in the diagram of the unit cell contents in Fig. S15. Quite distinct supramolecular association is evident in the crystal of **4** with hydrogen bonding interactions formed between the hydroxyl-O–H atoms and the carbonyl-O atoms of symmetry-related molecules indicating the hydroxyl-O–H hydrogen atoms are bifurcated owing to their participation in intramolecular hydroxyl-O–H…O(carbonyl) hydrogen bonds. This is consistent with the relatively weak nature of the intermolecular hydrogen bonding. As shown in Fig. 2b, these interactions lead to a supramolecular chain and four-membered $\{\cdots HO\cdots\}_2$ synthons. Being propagated by 2_1-screw symmetry along the b-axis direction, the chain has a helical topology. The chains are sustained into a three-dimensional architecture by a variety of C–H$\cdots\pi$ interactions with methylene-, methyl- and Cp-H being donors and hydroxylbenzoate and Cp rings being acceptors, Table 3. A view of the unit cell contents is shown in Fig. S16.

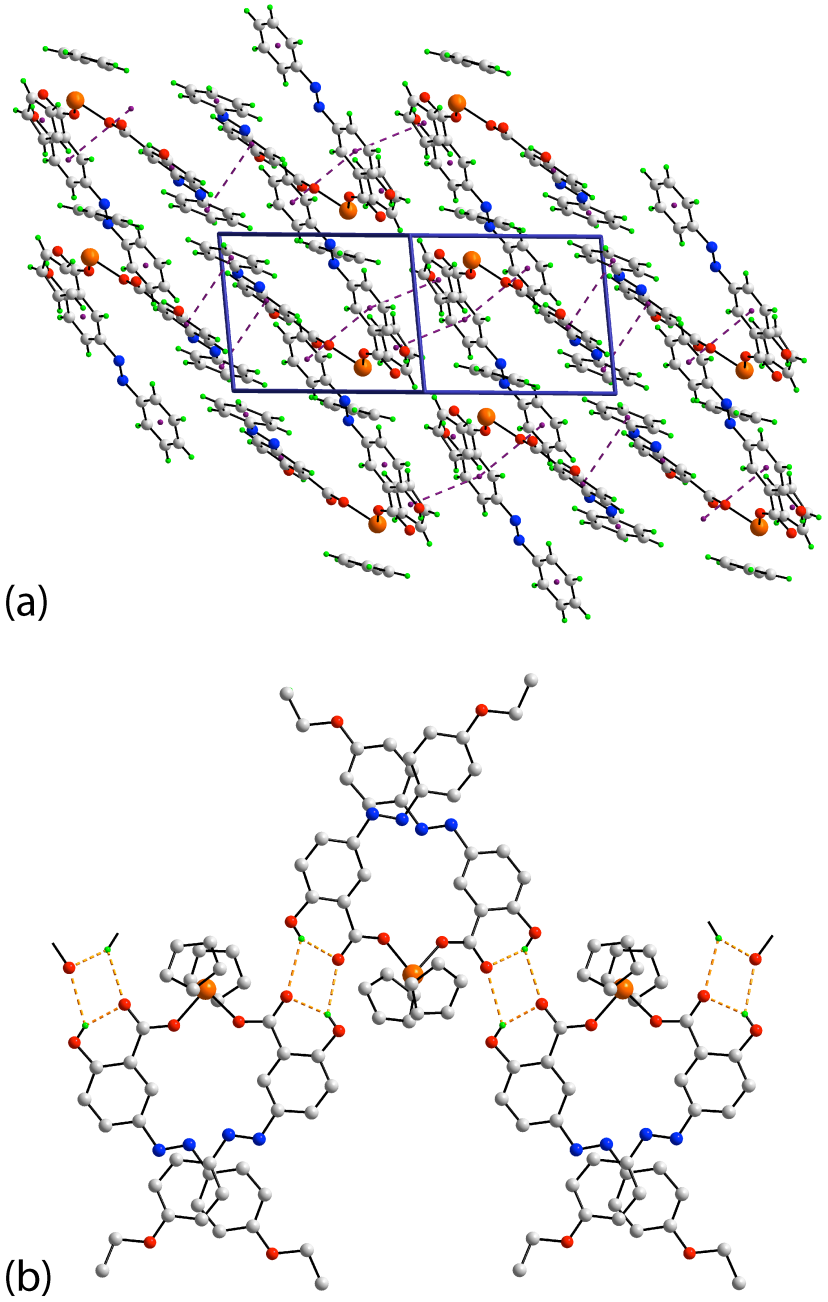

Fig. 2. Supramolecular association in the crystals of **3** and **4**: (a) **3**, a view of the supramolecular layer parallel to (0 1 1) sustained by π···π interactions (shown as purple dashed lines) and (b) **4**, a view of the supramolecular chain sustained by hydroxyl-O–H…O(carbonyl) hydrogen bonds (shown as orange dashed lines); non-participating hydrogen atoms are omitted for reasons of clarity.

The geometric parameters characterizing the supramolecular association operating in the crystals of **5**-**9** are summarised in Table 4. In the molecular packing of **5**, C–H···O(carbonyl) interactions feature prominently with the carbonyl-O2 atom accepting three such interactions from two Cp rings to generate a supramolecular chain along the b-axis, Fig. 3a. In essence, two Cp rings of one molecule of **5** connect to a carbonyl-O2 of a symmetry-related molecule and a second Cp-H atom of the original molecules connects to a second symmetry-related molecule to form a chain with a helical topology (2_1 screw symmetry). The main connections between chains are π···π stacking between hydroxybenzoate and Cp rings to form supramolecular layers that stack along the a-axis without directional interactions between them, at least based on the distance criteria assumed in PLATON [68]; a view of the unit cell contents is shown in Fig. S17. In **6**, a linear supramolecular chain along the b-axis is again formed through the agency of Cp-C–H···O(carbonyl) interactions, again with the carbonyl-O2 atom accepting three contacts, Fig. 3b. While the pattern of Cp-C–H···O(carbonyl) interactions in **6** matches that described for **5**, the difference is that in **6**, the chain is propagated by translational symmetry. As highlighted in Fig. S18, the chains are consolidated into the three-dimensional arrangement by π···π interactions between centrosymmetrically-related Cp rings and parallel C–F···π(hydroxybenzoate) interactions. Despite having a chlorophenyl group, the crystal of **7** is isostructural with **5** rather than with **6**. Thus, a helical supramolecular chain is formed along the b-axis, Fig. S19a, and supramolecular layers are formed in the bc-plane by π···π stacking interactions between hydroxybenzoate and Cp rings. The difference between **5** and **7** arises as directional interactions, i.e. of the type parallel C–Cl···π(hydroxybenzoate), occur between layers to establish the three-dimensional molecular packing, Fig. S19b. Distinctive packing patterns are found in the crystals of **8** and **9**.

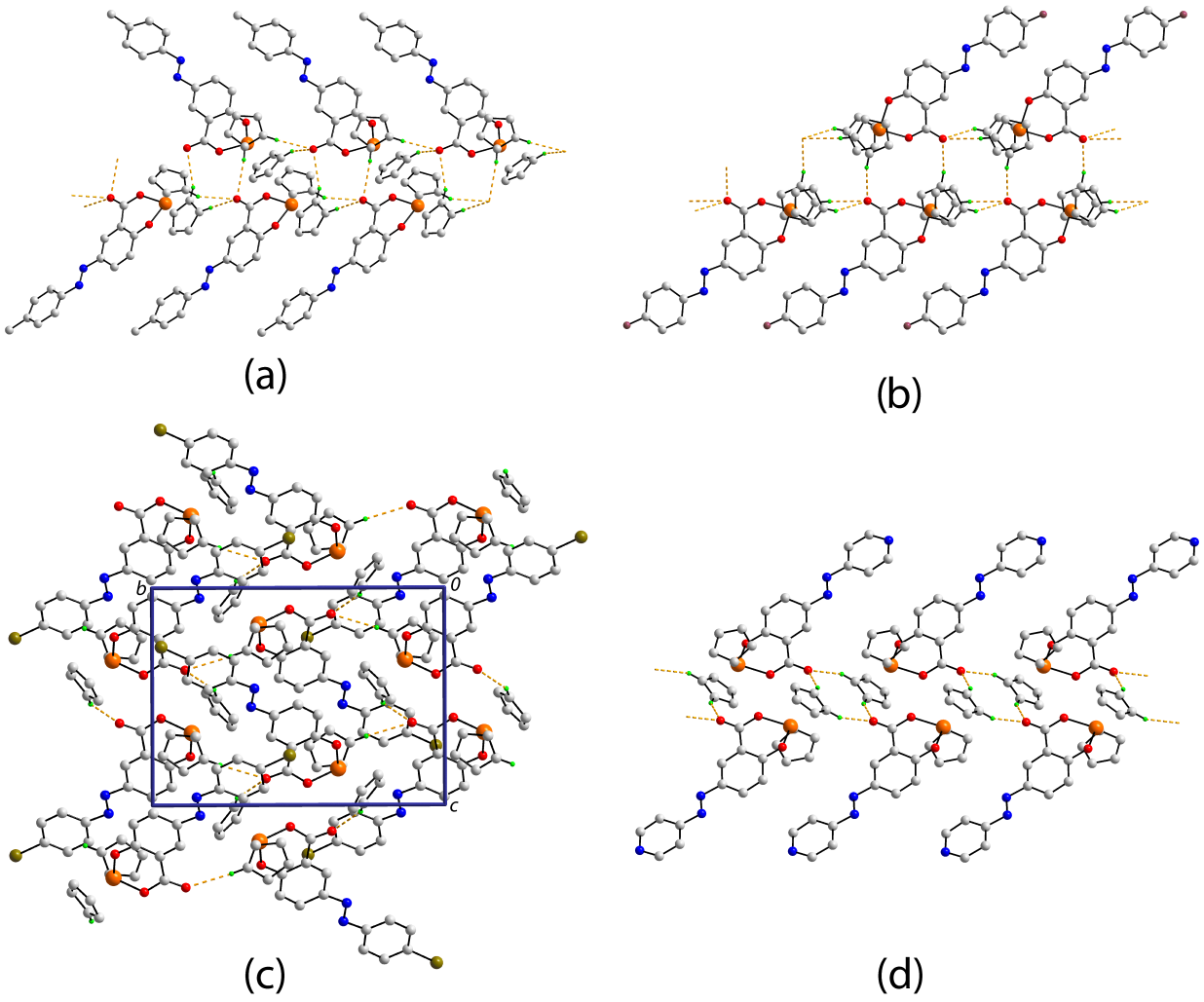

Fig. 3. Views of the supramolecular association sustained Cp-C–H···O(carbonyl) interactions in the crystals of **5**, **6**, **8** and **9**: (a) **5**, helical chain, (b) **4**, linear chain, (c) **8**, layer parallel to (0 1 1) and (d) **9**, linear chain. The Cp-C–H···O(carbonyl) interactions are shown as orange dashed lines and non-participating hydrogen atoms are omitted for reasons of clarity.

In the molecular packing of **8**, the carbonyl-O2 atom accepts two C–H···O(carbonyl) interactions with the donors derived from two symmetry-related molecules. As these interactions extend laterally, a supramolecular layer ensures, Fig. 3c. These stack along the c-axis being connected by hydroxybenzoate-C–H···π(bromophenyl) and parallel C–Br···π(hydroxybenzoate) interactions, Table 4 and Fig. S20. The only identifiable intermolecular interactions in the crystal of **9** are C–H···O(carbonyl) interactions whereby the carbonyl-O2 atom accepts two contacts derived from two symmetry-related molecules to sustain a linear supramolecular chain, Fig. 3d. A view of the unit cell contents is shown in Fig. S21. While no formal role for the pyridyl-nitrogen atom is noted, it is proximate to a symmetry-related Cp-H atom, being separated by 2.67 Å.

In summary, the crucial role of C–H···O(carbonyl) interactions in stabilising supramolecular chains in the crystals of **5-9** is established. The topology of the chain, helical (**5**, **7** and **8**) or linear (**6** and **9**) is dependent on the space group symmetry, Table 1. The presence of halide substituents in **6-8** ensures higher dimensionality of the supramolecular architectures through their participation in C–X···π interactions.

4. Conclusions

Several new members of bis(η^5-cyclopentadienyl)titanium(IV) arylazosalicylates were synthesised by conventional synthetic routes in anaerobic conditions in benzene. The compounds were characterised by IR and ^{1}H and ^{13}C NMR spectroscopic methods. The bulk samples of **3-9** were found to be consistent with their solid-state structures as revealed from NMR spectroscopy. The general solid-state constructs of **3-9** appear to be maintained in $CDCl_3$ solutions at least for couple of hours. X-ray crystallography established the stoichiometry of **3** and **4** as $Cp_2Ti(HL^{XASA}\text{-}\kappa O)_2$ and those of **5-9** as $Cp_2Ti(L^{XASA}\text{-}\kappa^2 O^1,O^2)$ with the molecular structures being based on distorted tetrahedral geometries based $(Cp)_2O_2$ donor sets and to be

largely independent of the nature of the substituents in the terminal phenyl rings. The molecular packing in **3** is based on π···π interactions but hydroxyl-O–H···O(carbonyl) bonding leads to supramolecular chains in **4**. In **5-9**, Cp-C–H···O(carbonyl) interactions persist and lead to supramolecular chains with helical (**5**, **7** and **8**) or linear (**6** and **9**) topologies; C–X···π interactions play an important role in the packing of **6-8**.

Conflict of interest

The authors declare that they have no conflicts of interest with the contents of this article.

Supplementary materials

Crystallographic data for compounds **3-9** reported in this paper have been deposited with the Cambridge Crystallographic Data Centre (CCDC) as supplementary publication nos. CCDC-1850180-CCDC-1850186. These data can be obtained free of charge via www.ccdc.cam.ac.uk/getstructures. ESI file contains the (a) **Figs. S1-S14**. ^{1}H NMR and ^{13}C NMR spectra of compounds **3-9**, respectively. (b) (i) **Fig. S15.** A view of the unit cell contents of **3** in projection down the a-axis highlighting the stacking of supramolecular layers. The π···π interactions are shown as purple dashed lines. (ii) **Fig. S16.** A view of the unit cell contents of **4** in projection down the b-axis. The O–H···O hydrogen bonding and C–H···π interactions are shown as orange and purple dashed lines, respectively. (iii) **Fig. S17.** A view of the unit cell contents of **5** in projection down the b-axis. The C–H···O and π···π interactions are shown as orange and purple dashed lines, respectively. (iv) **Fig. S18.** A view of the unit cell contents of **6** in projection down the b-axis. The C–H···O, π···π and C–H···F interactions are shown as

orange, purple and blue dashed lines, respectively. (v) **Fig. S19.** (a) a view of the supramolecular chain in **7** sustained by C–H…O(carbonyl) interactions; non-participating hydrogen atoms are omitted for reasons of clarity, and (b) a view of the unit cell contents of **7** in projection down the b-axis. The C–H···O, π···π and C–H···Cl interactions are shown as orange, purple and blue dashed lines, respectively. (vi) **Fig. S20.** A view of the unit cell contents of **8** in projection down the c-axis. The C–H···O, π···π and C–H···Br interactions are shown as orange, purple and blue dashed lines, respectively. (vii) **Fig. S21.** A view of the unit cell contents of **9** in projection down the b-axis. The C–H···O interactions are shown as orange dashed lines.

Acknowledgements

Financial support from the University Grants Commission, New Delhi (Grant No. Sanction No. 42-396/2013 (SR) Dated 25th March, 2013, TSBB) and the University Grants Commission, New Delhi, India through SAP-CAS, Phase-I (Grant No. F 540/21/CAS/2013 (SAP-I) are gratefully acknowledged. TSBB and RM acknowledge DST-PURSE for the diffractometer facility.

Table 1

Crystal data and refinement details for compounds **3**-**9**.

Compound	**3**	**4**	**5**	**6**	**7**
Formula	$C_{36}H_{28}N_4O_6Ti$	$C_{40}H_{36}N_4O_8Ti$	$C_{24}H_{20}N_2O_3Ti$	$C_{23}H_{17}FN_2O_3Ti$	$C_{23}H_{17}ClN_2O_3Ti$
Formula weight	660.52	748.63	432.32	436.28	452.73
Crystal colour	Orange	Orange	Dark-orange	Dark-red	Dark-red
Crystal size/mm^3	0.21 x 0.21 x 0.25	0.22 x 0.26 x 0.28	0.08x 0.09 x 0.15	0.09 x 0.09 x 0.25	0.21 x 0.25 x 0.26
Crystal system	Triclinic	Monoclinic	Monoclinic	Triclinic	Monoclinic
Space group	$P\bar{1}$	$P2_1/c$	$P2_1/c$	$P\bar{1}$	$P2_1/c$
a/Å	7.5735(6)	15.3444(6)	7.9077(2)	7.9774(4)	7.8967(7)
b/Å	14.0769(12)	17.0218(6)	8.8807(2)	8.8773(4)	8.8897(9)
c/Å	15.0774(13)	14.0822(8)	28.7042(6)	13.7253(7)	28.644(2)
[illegible]	76.955(7)	90	90	85.038(4)	90

β/°	85.748(7)	98.493(5)	91.637(2)	81.644(4)	91.894(7)
γ/°	78.948(7)	90	90	87.753(4)	90
V/Å^3	1535.5(2)	3637.8(3)	2014.96(8)	957.72(8)	2009.7(3)
Z	2	4	4	2	4
D_c/g cm^{-3}	1.429	1.367	1.425	1.513	1.496
F(000)	684	1560	896	448	928
μ/mm^{-1}	0.334	0.295	3.837	0.485	0.587
Measured data	12263	18513	7278	7227	8875
θ range/°	3.0 – 28.8	2.9 – 28.8	3.1 – 71.3	3.2 – 28.8	3.1 – 28.8
Unique data	6978	8273	3843	4282	4550
Observed data ($I \geq 2.0\sigma(I)$)	4098	5455	3255	3537	2316
No. parameters	430	486	272	271	271
R, obs. data; all data	0.076; 0.136	0.055; 0.095	0.042; 0.052	0.047; 0.060	0.081; 0.164

a; *b* in weighting scheme	0.066; 1.344	0.058; 0.633	0.050; 0.193	0.055; 0.523	0.090; 0.511
R_w, obs. data; all data	0.171; 0.202	0.119; 0.138	0.096; 0.101	0.112; 0.120	0.180; 0.226
GoF	1.05	1.03	1.05	1.03	1.00
Range of residual electron density peaks/eÅ^{-3}	-0.24 – 0.47	-0.27 – 0.23	-0.24 – 0.31	-0.28 – 0.52	-0.45 – 1.17

Table 1 cont.

Compound	**8**	**9**
Formula	$C_{23}H_{17}BrN_2O_3Ti$	$C_{22}H_{17}N_3O_3Ti$
Formula weight	497.19	419.28
Crystal colour	Dark-orange	Maroon
Crystal size/mm^3	0.25 x 0.26 x 0.29	0.19 x 0.19 x 0.21
Crystal system	Monoclinic	Triclinic
Space group	$P2_1/c$	$P\bar{1}$
a/Å	11.464(3)	7.9997(4)
b/Å	15.566(3)	8.9354(4)
c/Å	11.788(3)	13.3310(8)
α/°	90	85.090(4)
β/°	101.32(2)	78.659(5)

γ/°	90	82.736(4)
V/Å^3	2062.6(8)	924.99(9)
Z	4	2
D_c/g cm^{-3}	1.601	1.505
F(000)	1000	432
μ/mm^{-1}	2.380	0.493
Measured data	4668	7018
θ range/°	3.1 – 28.7	3.1 – 28.7
Unique data	4668	4152
Observed data ($I \geq 2.0\sigma(I)$)	1935	3513
No. parameters	272	262
R, obs. data; all data	0.091; 0.205	0.046; 0.057
a; b in weighting scheme	0.114; 0	0.058; 0.559

R_w, obs. data; all data	0.210; 0.285	0.116; 0.123
GoF	0.99	1.02
Range of residual electron density peaks/eÅ^{-3}	-0.77 – 0.83	-0.26 – 0.44

Table 2

Geometric parameters (Å, °) for molecular structures **3-9**.

Compound	**Ti–O1, O(y)**	**Ti–Cg1, Cg2** [a]	**O1–Ti–O(y)**	**Cg1–Ti–Cg2**	**Cp1/Cp2 dihedral**	**CO_2/C_6 dihedral**	**C_6/C_6 dihedral**
3, y = 4	1.947(3), 1.952(3)	2.049(3), 2.058(2)	90.24(12)	131.69(12)	51.0(3)	5.1(8), 3.9(8)	2.5(3), 15.6(2)
4, y = 4	1.9637(15), 1.9572(16)	2.0590(15), 2.0576(15)	88.71(6)	132.37(6)	49.0(2)	6.1(4), 11.85(14)	10.60(10), 7.23(7)
5, y = 3	1.9681(14), 1.9223(13)	2.0712(12), 2.0611(14)	87.46(6)	131.91(5)	50.67(16)	8.1(3)	15.83(12)
6, y = 3	1.9601(15), 1.9306(16)	2.0713(17), 2.0709(14)	87.05(7)	132.29(7)	50.7(2)	1.9(4)	12.10(15)
7, y = 3	1.954(4), 1.918(3)	2.073(3), 2.060(3)	87.84(16)	131.49(14)	50.5(4)	10.0(7)	16.9(3)
8, y = 3	1.943(5),	2.054(5),	87.1(2)	132.5(2)	49.3(7)	11(2)	6.2(5)

	1.922(6)	2.061(5)					
9, y = 3	1.9552(15), 1.9308(17)	2.0667(16), 2.0647(18)	87.13(7)	133.01(7)	51.0(2)	5.5(4)	18.01(14)

[a] Cg1 represents the ring centroid of the cyclopentadienyl ring with the lowest C-atom label.

Table 3

Geometric parameters (Å, °) characterising intra- and intermolecular interactions

A	H	B	H···B	A···B	A–H···B	Symme
3						
O3	H3o	O2	1.78(7)	2.535(6)	153(6)	x, y, z
O6	H6o	O5	1.79(6)	2.552(6)	153(5)	x, y, z
Cg(C32-C36)	–	Cg(C2-C7)	–	3.610(3)	2.5(3)[a]	1-x, 1-y
Cg(C2-C7)	–	Cg(C8-C13)	–	3.853(3)	2.5(2)	1+x, y,
Cg(C15-C20)	–	Cg(C21-C26)	–	3.804(3)	15.6(2)	1-x, -y,
4						
O3	H3o	O2	1.82(3)	2.567(2)	151(2)	x, y, z
O6	H6o	O5	1.84(3)	2.567(3)	149(3)	x, y, z
O3	H3o	O5	2.43(2)	3.037(2)	131(2)	-x, -½+
O6	H6o	O2	2.53(3)	3.144(3)	133(3)	-x, ½+y
C14	H14a	Cg(C2-C7)	2.90	3.783(4)	152	1-x, ½+
C29	H29a	Cg(C17-C22)	2.67	3.546(3)	151	1-x, -½-
C30	H30c	Cg(C36-C40)	2.88	3.834(4)	170	1+x, ½-
C36	H36	Cg(C31-C35)	2.90	3.678(3)	143	x, ½-y,

[a] Angle of inclination between the participating rings.

Table 4

Geometric parameters (Å, °) characterising intermolecular interactions in **5-9**.

A	H	B	H···B	A···B	A–H···B	Symmetry operation
5						
C18	H18	O2	2.59	3.444(3)	153	1-x, ½+y, 1½-z
C19	H19	O2	2.46	3.373(3)	169	x, 1+y, z
C22	H22	O2	2.58	3.372(3)	143	x, 1+y, z
Cg(C15-C19)	–	Cg(C8-C13)	–	3.9181(15)	10.49(13)[a]	1-x, 1-y, 1-z
6						
C18	H18	O2	2.51	3.371(4)	154	x, 1+y, z
C19	H19	O2	2.45	3.343(3)	161	1-x, 1-y, 1-z
C20	H20	O2	2.54	3.467(3)	172	x, 1+y, z
Cg(C14-C18)	–	Cg(C14-C18)	–	3.985(3)	0[a]	-x, 2-y, 1-z
C11	F1	Cg(C2-C7)	3.549(3)	3.855(3)	92.43(17)	-x, -y, -z
7						
C17	H17	O2	2.59	3.434(7)	151	1-x,1/2+y,3/2-z
C18	H18	O2	2.45	3.372(8)	170	x, 1+y, z
C20	H20	O2	2.54	3.353(8)	147	x, 1+y, z
Cg(C14-C18)	–	Cg(C8-C13)	–	3.936(4)	11.3(3)[a]	1-x, 1-y, 1-z
C11	Cl1	Cg(C2-C7)	3.609(3)	3.931(7)	87.2(2)	2-x, -y, 1-z
8						

C17	H17	O2	2.50	3.343(14)	152	-x, 1-y, 2-z
C20	H20	O2	2.54	3.469(13)	175	-x, -½+y, 1½-z
C4	H4	Cg(C14-C18)	2.91	3.729(10)	147	x, ½-y, -½+z
C11	Br1	Cg(C2-C7)	3.936(4)	4.000(11)	78.0(3)	x, 1½-y, -½+z
9						
C18	H18	O2	2.53	3.391(4)	154	-x, 1-y, 1-z
C19	H19	O2	2.49	3.334(4)	151	x, -1+y, z

[a] Angle of inclination between the participating rings.

References

[1] D.J. Ramón, M. Yus, Chem. Rev. 106 (2006) 2126-2208.

[2] S.A. Ryken, L.L. Schafer, Acc. Chem. Res. 48 (2015) 2576-2586.

[3] a) E. Le Roux, Coord. Chem. Rev. 306 (2016) 65-85;

b) L. Azor, C. Bailly, L. Brelot, M. Henry, P. Mobian, S. Dagorne, Inorg. Chem. 51 (2012) 10876-10883.

[4] R.A. Collins, A.F. Russell, P. Mountford, Appl. Petrochem. Res. 5 (2015) 153-171.

[5] S.C. Gagieva, V.A. Tuskaev, I.V. Fedyanin, M.I. Buzin, V.G. Vasil'ev, G.G. Nikiforova, E. S. Afanas'ev, S.V. Zubkevich, D.A. Kurmaev, N.A. Kolosov, E.S. Mikhaylik, E.K. Golubev, A.I. Sizov, B.M. Bulychev, J. Organomet. Chem. 828 (2017) 89-95.

[6] N.A. Kolosov, V.A. Tuskaev, S.C. Gagieva, I.V. Fedyanin, V.N. Khrustalev, O.V. Polyakova, B.M. Bulychev, Eur. Polym. J. 87 (2017) 266-276.

[7] S. Lee, S.S. Park, J.G. Kim, C.S. Kim, B.Y. Lee, Molecules, 22 (2017) 258 (pp. 1-15).

[8] H. Wang, X. Wang, Y. Sun, H. Cheng, T. Shiono, Z. Cai, Polymers 9 (2017) 131 (pp. 1-8)

[9] J.A. Garden, A.J.P. White, C.K. Williams, Dalton Trans. 46 (2017) 2532-2541.

[10] L.R. Doyle, A.J. Wooles, L.C. Jenkins, F. Tuna, E.J.L. McInnes, S.T. Liddle, Angew. Chem. Int. Ed. 57 (2018) 6314-6318.

[11] H. Assi, G. Mouchaham, N. Steunou, T. Devic, C. Serre, Chem. Soc. Rev. 46 (2017) 3431-3452.

[12] H.L. Nguyen, New J. Chem. 41 (2017) 14030-14043.

[13] J. Zhu, P.-Z. Li, W. Guo, Y. Zhao, R. Zou, Coord. Chem. Rev. 359 (2018) 80-101.

[14] M. Albrecht, I. Janser, S. Kamptmann, P. Weis, B. Wibbeling, R. Fröhlich, Dalton Trans. (2004) 37-43.

[15] M. Albrecht, I. Janser, A. Lützen, M. Hapke, R. Fröhlich, P. Weis, Chem. – Eur. J. 11 (2005) 5742-5748.

[16] Y. Sakata, S. Hiraoka, M. Shionoya, Chem. –Eur. J. 16 (2010) 3318-3325.

[17] C. Diebold, P. Mobian, C. Huguenard, L. Allouche, M. Henry, Inorg. Chem. 49 (2010) 6369-6371.

[18] D.M. Weekes, C. Diebold, P. Mobian, C. Huguenard, L. Allouche, M. Henry, Chem. – Eur. J. 20 (2014) 5092-5101.

[19] P. Mobian, N. Baradel, N. Kyritsakas, G. Khalil, M. Henry, Chem. – Eur. J. 21 (2015) 2435-2441.

[20] U. Schubert, J. Mater. Chem. 15 (2005) 3701-3715.

[21] K. Margulis-Goshen, S. Magdassi, Nanomedicine 5 (2009) 274-281.

[22] Y. Sang, B. Geng, J. Yang, Nanoscale 2 (2010) 2109-2113.

[23] K. Sabyrov, N.D. Burrows, R.L. Penn, Chem. Mater. 25 (2013) 1408-1415.

[24] H. Xu, S. Ouyang, P. Li, T. Kako, J. Ye, ACS Appl. Mater. Interfaces 5 (2013) 1348-1354.

[25] G. Cheng, Y. Wei, J. Xiong, Y. Gan, J. Zhua, F. Xu, Inorg. Chem. Front. 4 (2017) 1319-1329.

[26] H. Wang, H. Lin, Y. Long, B. Ni, T. He, S. Zhang, H. Zhu, X. Wang, Nanoscale 9 (2017) 2074-2081.

[27] W. Macyk, K. Szaciłowski, G. Stochel, M. Buchalska, J. Kuncewicz, P. Łabuz, Coord.

Chem. Rev. 254 (2010) 2687-2701.

[28] W. Fang, M. Xing, J. Zhang, J. Photichem. Photobiol. C: Photochem. Rev. 32 (2017) 21-39.

[29] E. Melendez, Crit. Rev. Oncol. Hematol. 42 (2002) 309-315.

[30] F. Caruso, M. Rossi, in: A. Sigel, H. Sigel (Eds.), Metal Ions in Biological System, Vol. 42, Metal Complexes in Tumor Diagnostics and as Anticancer Agents; Marcel Dekker, New York, USA, 2004.

[31] J.C. Dabrowiak, Metals in Medicine, Wiley, West Sussex, 2009.

[32] U. Olszewski, G. Hamilton, Med. Chem. 10 (2010) 302-311.

[33] K. Strohfeldt, M. Tacke, Chem. Soc. Rev. 37 (2008) 1174-1187.

[34] E.Y. Tshuva, D. Peri, Coord. Chem. Rev. 253 (2009) 2098-2115.

[35] G. Ramos, Y. Loperena, G. Ortiz, A. Szeto, J. Vera, J. Velez, J. Morales, D. Morrero, L. Castillo, S. Dharmawardhane, E. Melendez, A.V. Washington, Anticancer Res. 34 (2014) 1609-1615.

[36] L.M. Gao, W. Maldonado, X. Narváez-Pita, J.A. Carmona-Negrón, J. Olivero-Verbel, E. Meléndez, Inorganics, 4 (2016) 38; doi:10.3390/inorganics4040038

[37] E.Y. Tshuva, M. Miller, in: A. Sigel, H. Sigel, E. Freisinger, R.K.O. Sigel (Eds.), Coordination Complexes of Titanium(IV) for Anticancer Therapy, Chapter 8, Metallo-Drugs: Development and Action of Anticancer Agents, De Gruyter, Berlin, 2018.

[38] a) D. Pérez-Quintanilla, S. Gómez-Ruiz, Ž. Žižak, I. Sierra, S. Prashar, I. del Hierro, M. Fajardo, Z.D. Juranić, G.N. Kaluđerović, Chem. Eur. J. 15 (2009) 5588-5597;

b) G.N. Kaluđerović, D. Pérez-Quintanilla, I. Sierra, S. Prasar, I. del Hierro, Ž. Žižak, M. Fajardo, S. Gómez-Ruiz, J. Mater. Chem. 20 (2010) 806-814;

c) A. García-Peñas, S. Gómez-Ruiz, D. Pérez-Quintanilla, R. Paschke, I. Sierra, S. Prashar, I. del Hierro, G.N. Kaluđerović, J. Inorg. Biochem. 106 (2012) 100-110;

d) J. Ceballos-Torres, P. Virag, M. Cenariu, S. Prashar, M. Fajardo, E. Fischer-Fodor, S. Gómez-Ruiz, Chem. Eur. J. 20 (2014) 10811-10828;

e) W.A. Wani, S. Prashar, S. Shreaz, S. Gómez-Ruis, Coord. Chem. Rev. 312 (2016) 67-98;

f) S. Gómez-Ruiz, A. García-Peñas, S. Prashar, A. Rodríguez-Diéguez, E. Fischer-Fodor, Materials, 11, 224 (2018); doi:10.3390/ma11020224.

[39] M. Cini, T.D. Bradshaw, S. Woodward, Chem. Soc. Rev. 46 (2017) 1040-1051.

[40] M.R. Zierden, A.M. Valentine, Metallomics 8 (2016) 9-16.

[41] A. Tzubery, N. Melamed-Book, E.Y. Tshuva, Dalton Trans. 47 (2018) 3669-3673.

[42] R.-H. Wu, M. Guo, M.-X. Yua, L.-G. Zhu, Dalton Trans. 46 (2017) 14348-14355.

[43] L. Ni, D. Liang, Y. Cai, G. Diao, Z. Zhou, Dalton Trans. 45 (2016) 7581-7588.

[44] J.L. Hou, W. Luo, Y.Y. Wu, H.C. Su, G.L. Zhang, Q.Y. Zhu, J. Dai, Dalton Trans. 44 (2015) 19829-19835.

[45] J.D. Sokolow, E. Trzop, Y. Chen, J. Tang, L.J. Allen, R.H. Crabtree, J.B. Benedict, P. Coppens, J. Am. Chem. Soc. 134 (2012) 11695-11700.

[46] S. Eslava, A.C. Papageorgiou, S.K. Beaumont, G. Kyriakou, D.S. Wright, R.M. Lambert, Chem. Mater. 22 (2010) 5174-5178.

[47] K. Shirakawa, L. Wang, N. Man, J. Maksimoska, A.W. Sorum, H.W. Lim, I.S. Lee, T. Shimazu, J.C. Newman, S. Schröder, M. Ott, R. Marmorstein, J. Meier, S. Nimer, E. Verdin, eLife, 5 (2016) e11156; doi: 10.7554/eLife.11156

[48] G. Huang, H. Cheng, Y. Liu, J. Hu, Saudi Pharm. J. 26 (2018) 263-265.

[49] Z.-Q. Hang, S.-W. Lu, H.-F. Guo Dalian, Z.-R. Lu, Y.-K. Zhou, Synth. React. Inorg. Met.-Org. Chem. 22 (1992) 883-892.

[50] M.G. Meirim, E.W. Neuse, M. Rhemtula, S. Schmitt, H.H. Brintzinger, Transition Met. Chem. 13 (1988) 272-276.

[51] D.A. Edwards, M.F. Mahon, T.J. Paget, N.W. Summerhill, Transition Met. Chem. 26 (2001) 116-119.

[52] Z.-W. Gao, D.-D. Hu, L.-X. Gao, X.-L. Zhang, Z.-T. Zhang, Q.-Q. Liang, J. Organomet. Chem. 629 (2001) 47-53.

[53] J. Li, Z. Gao, C. Zhang, L. Gao, J. Chem. Crystallogr. 39 (2009) 623-631.

[54] F. Xu, Z.-W. Gao, L.-X. Gao, J.-L. Li, Acta Crystallogr. Sect. E 62 (2006) m2811-m2812.

[55] J.-L. Li, Z.-W. Gao, L.-X. Gao, F. Xu, Acta Crystallogr. Sect. E 63 (2007) m460-m461.

[56] F. Xu, Z.-W. Gao, C.-Y. Zhang, L.-X. Gao, J.-L. Li, Acta Crystallogr. Sect. E 63 (2007) m540-m541.

[57] Z.-W. Gao, F. Xu, C.-Y. Zhang, L.-X. Gao, Acta Crystallogr. Sect. E 63 (2007) m542-m543.

[58] Y. Wu, C. Chen, G. Jia, X. Zhu, H. Sun, G. Zhang, W. Zhang, Z. Gao, Chem. Eur. J. 20 (2014) 8530-8535.

[59] T.S. Basu Baul, R. Manne, E.R.T. Tiekink, J. Coord. Chem.; DOI 10.1080/00958972.2018.1528355.

[60] T.S. Basu Baul, S. Dhar, S.M. Pyke, E.R.T. Tiekink, E. Rivarola, R. Butcher, F.E. Smith, J. Organomet. Chem. 633 (2001) 7-17.

[61] T.S. Basu Baul, S. Dhar, N. Kharbani, S.M. Pyke, R. Butcher, F.E. Smith, Main Group Met. Chem. 22 (1999) 413-421.

[62] T.S. Basu Baul, A. Chaurasiya, A. Duthie, M.G. Vasquez-Ríos, H. Höpfl, J. Organomet. Chem. 872 (2018) 87-101.

[63] Agilent Technologies, CrysAlisPro, Santa Clara, CA, USA, 2013.

[64] G.M. Sheldrick, Acta Crystallogr. Sect. A 64 (2008) 112-122.

[65] G.M. Sheldrick, Acta Crystallogr. Sect. C 71 (2015) 3-8.

[66] L.J. Farrugia, J. Appl. Crystallogr. 45 (2012) 849-854.

[67] DIAMOND, Visual Crystal Structure Information System, Version 3.1, Crystal Impact, Postfach 1251, D-53002 Bonn, Germany, 2006.

[68] A.L. Spek, Acta Crystallogr. Sect. D 65 (2009) 148-155.

[69] G.B. Deacon, R.J. Philips, Coord. Chem. Rev. 33 (1980) 227-250.

[70] C.R. Groom, I.J. Bruno, M.P. Lightfoot, S.C. Ward, Acta Crystallogr. Sect. B 72 (2016) 171-179.